Absolute refractive indices and thermal coefficients of CaF_2, SrF_2, BaF_2, and LiF near 157 nm

John H. Burnett, Rajeev Gupta, and Ulf Griesmann

We present high-accuracy measurements for wavelengths near 157 nm of the absolute index of refraction, the index dispersion, and the temperature dependence of the index for the ultraviolet optical materials with cubic symmetry: CaF_2, SrF_2, BaF_2, and LiF. Accurate values of these quantities for these materials are needed for designs of the lens systems for F_2 excimer-laser-based exposure tools for 157-nm photolithography. These tools are expected to use CaF_2 as the primary optical material and possibly one of the others to correct for chromatic aberrations. These optical properties were measured by the minimum deviation method. Absolute refractive indices were obtained with an absolute accuracy of 5×10^{-6} to 6×10^{-6}.

OCIS codes: 120.5710, 160.4670, 160.4760.

1. Introduction

Recent developments in semiconductor lithography with molecular fluorine (F_2) excimer lasers, emitting near 157 nm, have made it necessary to obtain accurate data for the refractive-index properties of optical materials near this wavelength. Designing and implementing precision 157-nm optics requires accurate values of the absolute index of refraction, the index dispersion ($dn/d\lambda$), and the temperature dependence of the index (dn/dT) at this wavelength for the optical materials used. Sample-to-sample variations of these properties must be known as well. The requirements that the materials be highly transparent near 157 nm, have isotropic optical properties, relatively low hygroscopicity, and good-quality polishing characteristics leave a short list of candidate materials, principally the cubic-symmetry fluorides CaF_2, SrF_2, BaF_2, and LiF. CaF_2 is generally considered the principal candidate, but to achromatize all-refractive optics over the F_2 laser bandwidth may require combination with at least a second material.

Accurate index data (uncertainty $\leq 1 \times 10^{-5}$) for CaF_2, by use of the minimum deviation method, are available for longer wavelengths. Malitson published refractive indices for CaF_2 for wavelengths from 9700 nm down to 230 nm.[1] Gupta *et al.* published CaF_2 data for wavelengths near 193 nm.[2] Index values for CaF_2, SrF_2, BaF_2, and LiF are available at lower accuracy for wavelengths down to their band edges in the compilation by Palik, taken from various sources referenced therein.[3] However, these latter values have uncertainties of the order of 1×10^{-3}, several orders of magnitude larger than required for lithography optics design. To our knowledge, there are no published index measurements for these materials near 157 nm with an accuracy in the required range of approximately 1×10^{-5} previous to this study.

In this paper we report accurate (absolute uncertainty $\approx 5 \times 10^{-6}$) measurements of the absolute index of refraction, the index dispersion ($dn/d\lambda$), and the temperature dependence of the index (dn/dT) near 157 nm for CaF_2, SrF_2, BaF_2, and LiF, as well as some sample-to-sample variations. [All uncertainties in this paper are combined standard ($k = 1$) uncertainties.[4]] These results are summarized in Table 1 of Section 3. We first describe in Section 2 the methods and procedures used to make the measurements. These are based on the minimum deviation method, which is commonly used to measure the indices of optical materials with high accuracy for visible and near-ultraviolet wavelengths. However, implementation of this method in the vacuum ultraviolet (VUV) region, where the oxygen component of air is highly absorbing, required substantial modifications of the usual procedures. The results are presented in Section 3 and discussed in Section 4.

The authors are with the National Institute of Standards and Technology, Building 221, Room B228, 100 Bureau Drive, Gaithersburg, Maryland 20899-8421. J. H. Burnett's e-mail address is john.burnett@nist.gov.

Received 20 November 2001; revised manuscript received 23 January 2002.

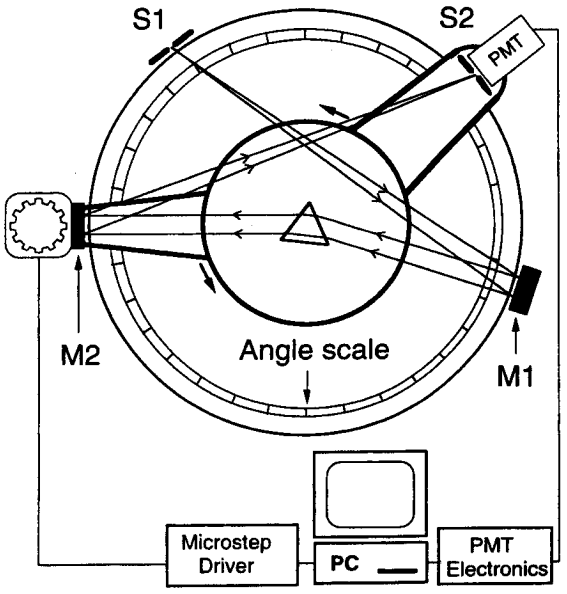

Fig. 1. Schematic of the UV goniometric spectrometer with reflective optics. S1 and S2 are the entrance and exit slits, respectively; M1 is a collimating mirror and M2 a focusing mirror.

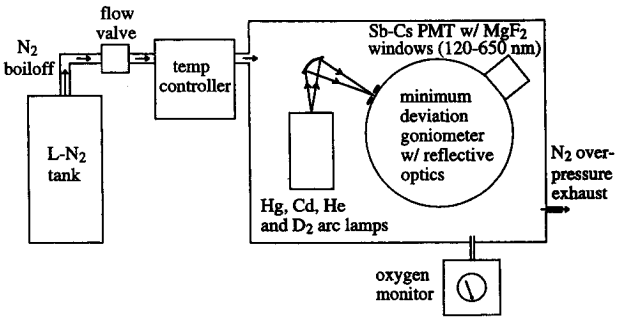

Fig. 2. Schematic of the UV goniometric spectrometer enclosed in a temperature-controlled N_2 gas purge housing for index measurements near 157 nm.

2. Measurement Procedure

Our procedure was based on the minimum deviation technique.[5,6] In this method a prism of the material is fabricated with a nominal apex angle A, which is accurately measured. One measures the deviation angle D of monochromatic light of wavelength λ as it passes through the prism. If the prism is oriented symmetrically with respect to the incident and transmitted light, the deviation is at a minimum and the absolute index of the material n_{mat} at the wavelength λ is given by Eq. (1) shown below. n_{mat} depends at the wavelength λ only on the minimum deviation angle $D(\lambda)$, the apex angle A, and the index of the surrounding gas n_{gas}.

$$n_{\mathrm{mat}}(\lambda) = \frac{\sin\left[\frac{A + D(\lambda)}{2}\right]}{\sin\left(\frac{A}{2}\right)} n_{\mathrm{gas}}(\lambda). \qquad (1)$$

Our implementation of the minimum deviation method for wavelengths in the UV is indicated schematically in Fig. 1, which shows a goniometric spectrometer with all-reflective optics.[2] A prism of the material with a nominal apex angle A of 60° is mounted on the turntable of the goniometric spectrometer as indicated in Fig. 1. The beam of a He–Ne laser, which enters the goniometer through the entrance slit S1, is used to align the prism so as to achieve a minimum in the deviation angle D. The turntable of the goniometer is then locked to a precise mechanical θ-to-2θ drive that maintains the minimum deviation alignment of the prism while focusing mirror M2 and exit slit S2 are scanned from one spectral line to the next with a stepper motor and precision gears. A Sb–Cs photomultiplier tube (PMT) detector with MgF_2 windows, sensitive in the region ≈120–650 nm, is mounted behind exit slit S2. The refractive index of the prism material n_{mat} at a wavelength λ relative to the index of the surrounding gas medium n_{gas} is calculated with Eq. (1) once the apex angle A and the minimum deviation angle $D(\lambda)$ have been measured.

Because of mechanical limitations, it was not possible to observe the undeviated beam in this system. This spectrometer was therefore restricted to measurements of deviation angle differences for two wavelengths. We obtained absolute deviation angles for wavelengths near 157 nm by adding absolute deviation angles for visible spectral emission lines from He, Hg, and Cd spectral lamps, measured on a separate visible refractive goniometric spectrometer, to the relative deviations between these visible lines and deuterium arc lamp lines near 157 nm, measured on the UV goniometric spectrometer. We obtained the relative angular deviations by scanning the UV goniometric spectrometer between the visible lines and the deuterium lines near 157 nm using the stepper motor. Several scans were recorded on a computer, and we determined the angular position for each spectral line by fitting the recorded lines to Gaussians and taking the average of the Gaussian centers. The uncertainty of the minimum deviation angle measurements was 1.6 arc sec. We measured the apex angles of the prisms by mounting them on a different goniometer and making a series of measurements of the orientation angles of the prism faces with an autocollimator and comparing these with a calibrated reference angle. The standard deviation of an apex angle measurement was 0.24 arc sec.

Because O_2 absorbs strongly for wavelengths below approximately 185 nm,[7] the relative deviation measurements between the visible and the 157-nm wavelengths were made in a N_2 purge gas environment. As shown schematically in Fig. 2, the spectrometer and spectral line sources were enclosed in a sealed chamber with adjustable exhaust ports, purged with N_2 gas.[8] The N_2 gas flowed from the controlled boiloff from a liquid-N_2 tank. The residual O_2 content was monitored with an O_2 analyzer. Because

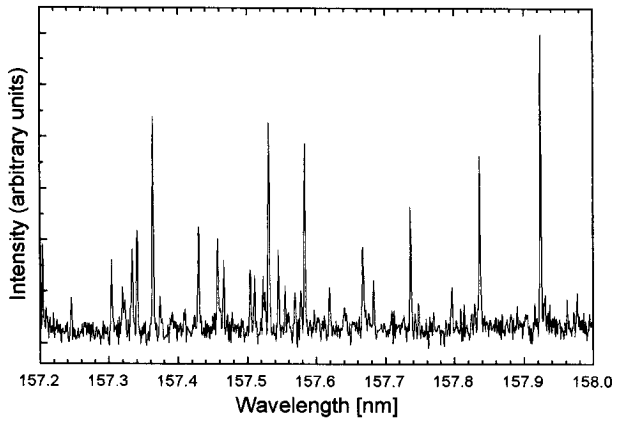

Fig. 3. Deuterium lamp spectrum near 157 nm taken with the NIST FT700 VUV Fourier-transform spectrometer. The wavelength accuracy is 0.02 pm; the instrumental resolution is 0.1 pm.

the absorption coefficient of O_2 near 157 nm is $k \approx 200\ \mathrm{cm}^{-1}\ \mathrm{atm}^{-1}$,[7] to obtain sufficient transmission near 157 nm over the ≈2-m optical path from the spectral line sources through the goniometer to the detector, we held the O_2 content below approximately 10 parts per million during the measurements. We controlled the gas and prism temperatures by first flowing the N_2 gas through a temperature bath with its temperature adjusted by a feedback control loop to the prism temperature, determined by several calibrated Si-diode thermometers. This procedure enabled temperature control to 0.05 °C.

The relative angular deviation measurements were made between six visible spectral emission lines from He, Hg, and Cd lamps and eight spectral emission lines in the range 156.8–158.6 nm from a low-pressure deuterium lamp. (Low-pressure deuterium lamps have strong, sharp spectra lines in the range of approximately 150–165 nm.) We obtained the wavelengths of these deuterium lines using the FT700 VUV Fourier-transform spectrometer that we developed at the National Institute of Standards and Technology (NIST).[9] A vacuum spectrum near 157 nm of our deuterium lamp taken with the Fourier-transform spectrometer is shown in Fig. 3. The wavelength accuracy was 0.02 pm, and the instrumental resolution was 0.1 pm. (Because the wavelengths of the peaks of the deuterium lamps vary somewhat between lamps, this calibration is valid only for this lamp.)

The absolute deviations of the visible lines were measured with the visible goniometric spectrometer in air with the temperature controlled and the pressure and humidity monitored. The 157-nm relative deviation measurements were made in a dry N_2 atmosphere with the pressure monitored and the temperature controlled to the temperature that was used to measure the visible wavelength deviations. We obtained the absolute angular deviations in N_2 gas of the eight spectral lines near 157 nm by adding the relative deviations between the visible and the 157-nm lines to the absolute deviations of the visible lines, corrected to the N_2 gas environment by using the visible air[10] and N_2 gas[11] refractive-index dispersion relations and Eq. (1). For each of the eight spectral lines measured near 157 nm, the index of refraction of the sample relative to N_2 gas at the temperature and pressure measured was obtained with Eq. (1) with the measured apex angle A and deviation angle $D(\lambda)$. We obtained the absolute indices of the eight spectral lines by multiplying the relative indices by the index of N_2 gas at the VUV wavelengths. We determined the index of N_2 gas interferometrically and include it below as Eq. (2).[12] The formula gives the index of N_2 gas, with a standard uncertainty of 0.2×10^{-6}, for λ in the range 145–270 nm for temperatures and pressures near standard conditions: $T = 0$ °C and $P = 1.01325$ bars (1.01325×10^5 Pa or 1 standard atmosphere). Here λ is in nanometers, T is in degrees Celsius, and P is in bars.

$$
\begin{aligned}
[n(\lambda) - 1]_{T,P} = [n(\lambda) - 1]_0 & \\
\times \left(\frac{P}{1.01325}\right) & \left(\frac{273.15}{273.15 + T}\right) \\
\times \left(\frac{0.9995555}{Z}\right) & \\
\times \left\{1 + \left[\frac{(n(\lambda) - 1)_0}{6}\right]\right. & \left[1 \right. \\
- \left(\frac{P}{1.01325}\right) & \left(\frac{273.15}{273.15 + T}\right)\left.\right]\Bigg\}^{-1},
\end{aligned}
\tag{2}
$$

where

$$
\begin{aligned}
[n(\lambda) - 1]_0 &= [n(\lambda) - 1]_{0\,^\circ\mathrm{C},\,1.01325\mathrm{bars}} \\
&= \frac{1.9662731}{22086.66 - (1000/\lambda)^2} \\
&\quad + \frac{0.027450825}{133.85688 - (1000/\lambda)^2}, \\
Z &= 1 - \left(\frac{P}{1.01325}\right)(44.45 - T) \times 10^{-5}.
\end{aligned}
$$

Finally, a least-squares quadratic was fit to the measured indices to determine the dispersion in the range from 156.8 to 158.6 nm with an absolute accuracy of $\sigma = 5 \times 10^{-6}$ to 6×10^{-6}.

The temperature of the prism, prism holder, and N_2 gas could be varied and controlled between 19 °C and 26 °C with an accuracy of 0.05 °C. This allowed us to measure the relative index of refraction of spectral lines near 157 nm at approximately 1 °C intervals. Separate measurements were made for increments in temperature in ascending and descending order. For each series a linear least-squares fit to the data was obtained to obtain dn/dT in N_2 gas, and the results for the two series were averaged. In all cases the deviation from the aver-

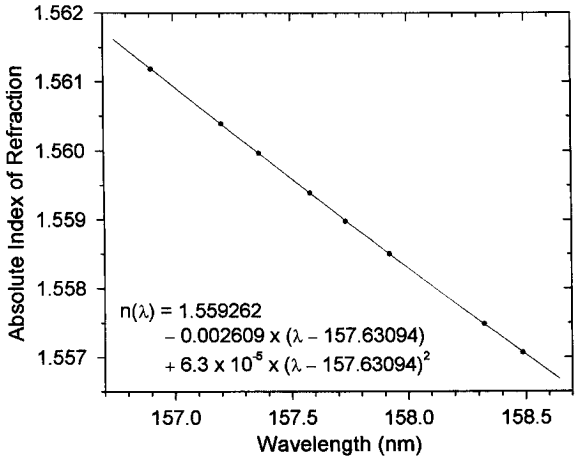

Fig. 4. Absolute refractive index of the CaF_2 sample C at 20.00(5) °C at eight deuterium lamp spectral line wavelengths in the range 156.8–158.6 nm. The curve is a quadratic least-squares fit to the data and is given by the inset formula. The first two coefficients give the index and dispersion at 157.63094 nm.

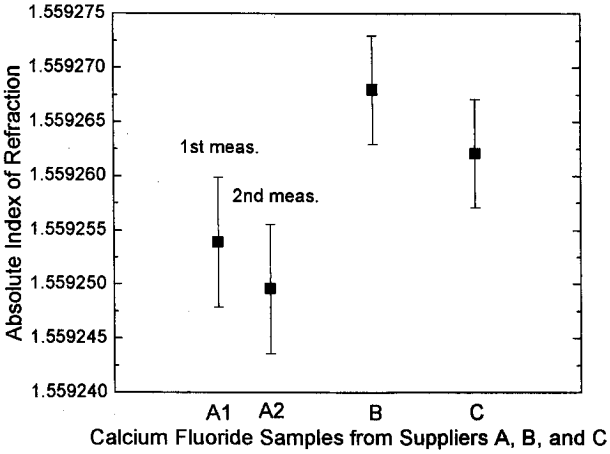

Fig. 5. Absolute refractive index of three samples of CaF_2 from three different suppliers at 20.00(5) °C and at 157.63094 nm. Sample A was measured twice independently. The error bars correspond to standard uncertainties of 6×10^{-6} for sample A and 5×10^{-6} for samples B and C. The results for sample C are included in Table 1.

age was less than the uncertainty of the linear least-squares fit. Correcting for the temperature dependence of the index of N_2 gas from Eq. (2) enabled us to determine the temperature coefficient of the absolute refractive index of the materials near 157 nm.

3. Results

The absolute index of refraction of three recently grown samples of calcium fluoride from three suppliers was measured for eight deuterium lamp spectral lines between 156.8 and 158.6 nm. The samples are labeled here A, B, and C. Sample A was measured twice independently. The measurements were made at slightly different temperatures near 20 °C, but they were all normalized to 20 °C with the temperature coefficient measured separately and discussed below. A quadratic polynomial was fit to the normalized data for each sample to obtain a dispersion curve near 157 nm. The normalized data for sample C along with the quadratic dispersion curve near 157 nm are shown in Fig. 4. The coefficients of the quadratic polynomial fit for this sample are given in the fifth column of Table 1. This dispersion relation has a standard uncertainty of $\sigma = 5 \times 10^{-6}$ over the range 156.8–158.6 nm. The dispersion curves for each sample were evaluated at the F_2 excimer laser vacuum wavelength 157.63094 nm,[13] and these results are shown for comparison in Fig. 5. The error bars for samples B and C correspond to a standard uncertainty of $\sigma = 5 \times 10^{-6}$. The error bars for

Table 1. Absolute Index, Dispersion, and Temperature Dependence of LiF, CaF_2, SrF_2, and BaF_2 near 157 nm[a]

Material	Absolute Index [20.00(5) °C] (157.63094 nm)	$dn/d\lambda$ (157.63094 nm) (nm^{-1})	dn/dT (near 20 °C) ($°C^{-1}$)	Coefficients of $n(\lambda) = a_0 + a_1(\lambda - 157.63094) + a_2(\lambda - 157.63094)^2$
LiF	$1.485152(6) \times 10^{-6}$	$-0.001711(7)$	0.4×10^{-6}/°C (vacuum) ($\pm 1.6 \times 10^{-6}$/°C) 2.2×10^{-6}/°C (N_2)	$a_0 = 1.485152$ $a_1 = -0.001711$ $a_2 = 3.6 \times 10^{-5}$
CaF_2 (three samples)	C: $1.559262(5) \times 10^{-6}$ average: 1.559261 spread: 16×10^{-6}	C: $-0.002609(4)$ average: -0.002607 spread: 6×10^{-6}	$6.1(3) \times 10^{-6}$/°C (vacuum) $8.0(3) \times 10^{-6}$/°C) (N_2)	Sample C: $a_0 = 1.559262$ $a_1 = -0.002609$ $a_2 = 6.3 \times 10^{-5}$
SrF_2	$1.575580(6) \times 10^{-6}$	$-0.003055(5)$	3.9×10^{-6}/°C (vacuum) ($\pm 1.5 \times 10^{-6}$/°C) 5.8×10^{-6}/°C (N_2)	$a_0 = 1.575580$ $a_1 = -0.003055$ $a_2 = 5.9 \times 10^{-5}$
BaF_2 (three samples)	D: $1.656684(6) \times 10^{-6}$ average: 1.656682 spread: 26×10^{-6}	D: $-0.004375(4)$ average: -0.004370 spread: 9×10^{-6}	$8.6(5) \times 10^{-6}$/°C (vacuum) $10.6(5) \times 10^{-6}$/°C (N_2)	Sample D: $a_0 = 1.656684$ $a_1 = -0.004375$ $a_2 = 1.05 \times 10^{-4}$

[a]Absolute index of refraction (column 1), dispersion (column 2), and temperature dependence of the index (column 3) at 157.63094 nm. The temperature is 20.00(5) °C. For CaF_2 and BaF_2 three samples were measured, and data are given for one sample each, along with the averages and spreads. The coefficients of quadratic polynomials that were fit to the refractive-index data between 156.8 and 158.6 nm are listed in the rightmost column for one sample of each material. The formula is valid in this range with the standard uncertainties given in column 1.

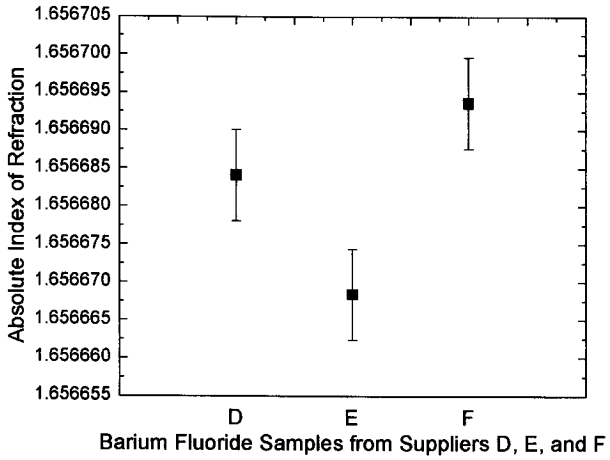

Fig. 6. Absolute refractive index of three samples of BaF_2 from three different suppliers at 20.00(5) °C and at 157.63094 nm. The error bars correspond to standard uncertainties of 6×10^{-6} for all samples. The results for sample D are included in Table 1.

sample A correspond to a standard uncertainty of $\sigma = 6 \times 10^{-6}$. Note that the index values for the three samples have a spread of 16×10^{-6}, suggesting a sample-to-sample index variation on this order.

The results for CaF_2 are summarized in the second data row of Table 1. The first data column gives the index and its uncertainty for sample C evaluated at 157.63094 nm, along with the average and spread of the indices for the three samples. The second column gives the dispersion ($dn/d\lambda$) and its uncertainty for sample C evaluated at 157.63094 nm, along with the average and spread for the three samples. The third column gives the temperature dependence (dn/dT) of the absolute index and its uncertainty near 157 nm and 20 °C for one CaF_2 sample determined as described in Section 2 above. Values are given for vacuum and for 1 atm of N_2 gas.

Using methods similar to those used for CaF_2, we also measured the absolute index of refraction, the index dispersion, and the temperature dependence of the index for three recently grown samples of BaF_2 labeled here D, E, and F. The results for the absolute index at 157.63094 nm and 20 °C for the three samples are shown in Fig. 6. The spread of the index values is 26×10^{-6}, well outside the error bars. The results are summarized in Table 1. Similar measurements were also made for one sample each of recently grown SrF_2 and LiF, and the results are summarized in Table 1.

The uncertainty of the absolute index measurements is stated in Table 1 as $\sigma = 5 \times 10^{-6}$ for two samples of CaF_2 and $\sigma = 6 \times 10^{-6}$ for the LiF, SrF_2, and BaF_2 samples. A number of factors contributed to the uncertainties, and these are summarized in Table 2. By far the dominant contribution to the net uncertainty comes from the uncertainty in the minimum deviation angle measurements, which cannot be significantly improved in our systems. These result from combined uncertainties of the deviation angles for the visible angle measurements and the relative angle measurements discussed above. The angles for both goniometers were determined from ruled scales in the instruments with previously determined absolute accuracies of 1 arc sec. Additional uncertainties were introduced by our scale reading procedures, which with averaging resulted in a net deviation angle uncertainty of 1.6 arc sec. This is consistent with the fact that values of the absolute UV deviation angles for a given wavelength determined by use of the different visible lines (with different regions of the goniometer scales) agreed within 1 arc sec, and these measurements were averaged. The next largest contribution to the uncertainty is from the intrinsic birefringence discussed in Section 4.

4. Discussion

LiF, CaF_2, SrF_2, and BaF_2 can all be grown as large, high-quality single crystals and have absorption edges deep in the VUV. They each have cubic symmetry [space group Fm3m (O_h^5)] and consequently have isotropic optical properties. For these reasons

Table 2. Uncertainty Budget for Refractive-Index Measurement

Source of Uncertainty	Value	Index Uncertainty
Apex angle A	0.24 arc sec	0.7×10^{-6}
Deviation angle D		
Visible goniometer deviation measurement uncertainty	1.1 arc sec	
Visible goniometer effect of temp., press., hum. uncertainty	0.1 arc sec	
UV goniometer deviation measurement uncertainty	1.2 arc sec	
Net deviation angle uncertainty	1.63 arc sec	4.9×10^{-6}
Wavelength λ	0.02 pm	0.1×10^{-6}
Index of N_2 gas n_{gas}		
Index uncertainty	0.2×10^{-6}	0.2×10^{-6}
Temperature uncertainty	0.05 °C	0.1×10^{-6}
Pressure uncertainty	1 bar	0.3×10^{-6}
Material temperature	0.05°	0.3×10^{-6}
Correction to 20 °C	0.05	0.6×10^{-6}
Intrinsic birefringence	$1(3) \times 10^{-6}$	$1(3) \times 10^{-6}$
Combined uncertainty[a]		$5.1(5.8) \times 10^{-6}$

[a]All uncertainties are standard ($k = 1$) uncertainties.

they are principal materials used for precision optics applications in the VUV, in particular for 157-nm lithography. The alkali halide LiF, with the cubic NaCl structure, has the largest-energy absorption edge. The alkaline earth fluorides CaF_2, SrF_2, and BaF_2, with the cubic fluorite structure, form a series in the order of increasing mass of the group II element and have decreasing absorption edge energies. The index results summarized in Table 1 of Section 3 are listed for the materials in this order of decreasing absorption edge energy. As might be expected, this trend correlates with larger indices and larger magnitudes of the dispersions for all the materials.

The indices of refraction are given with absolute accuracy of 5×10^{-6} to 6×10^{-6}, limited by the deviation angle measurement. Although improvement in this angle measurement could reduce this uncertainty somewhat, there is an inherent limitation on the significance of this type of measurement of an isotropic index value. In spite of the fact that these materials have cubic symmetry, they must actually have intrinsic birefringences at short wavelengths because of spatial dispersion.[14–16] It was recently shown that CaF_2 and BaF_2 have intrinsic birefringences at 157.63 nm of $1.12(4) \times 10^{-6}$ and $3.4(3) \times 10^{-6}$, respectively.[16] Our calculations of intrinsic birefringences near 157 nm for SrF_2 and LiF predict values also in this range. Thus, for measurements in this wavelength range with uncertainties much below our values, the materials must be considered birefringent, and appropriate modifications of the measurement procedures by use of polarizers must be made.

The temperature dependencies (dn/dT) listed in the third column of Table 1 are all positive at 157 nm, although the values are not in a monotonic sequence. For CaF_2 this value is negative at longer wavelengths [dn/dT (458 nm, 20 °C) = -11×10^{-6}/°C.[17]] This trend from negative values of dn/dT at longer wavelengths in the visible to positive values in the VUV holds for SrF_2, BaF_2, and LiF as well. [For SrF_2, dn/dT(458 nm, 20 °C) = -12×10^{-6}/°C; for BaF_2, dn/dT(458 nm, 20 °C) = -15.6×10^{-6}/°C; for LiF, dn/dT (458 nm, 20 °C) = -16×10^{-6}/°C.[17]]

Our index measurements have several implications for precision refractive optics design at 157 nm. The magnitude of the dispersion near 157 nm for LiF and BaF_2 is 34% smaller and 68% larger, respectively, than that of CaF_2. This may make LiF and BaF_2 good candidates for second materials to be combined with CaF_2 for chromatic aberration correction at 157 nm. Index measurements of three samples each of CaF_2 and BaF_2 show sample variations of 16×10^{-6} and 26×10^{-6}, respectively, well outside the index uncertainties of 5×10^{-6} to 6×10^{-6}. These sample index spreads suggest differences in material quality for even the best material available at this time and may have implications for design tolerances.

Partial funding for this project was received from International SEMATECH. Partial funding was also received from the Office of Microelectronics Programs at NIST, and we gratefully acknowledge Steven Knight of the Office of Microelectronics Programs for helpful discussions and continuous support. We also thank Bryon Faust at NIST for the apex angle measurements.

References

1. I. H. Malitson, "A redetermination of some optical properties of calcium fluoride," Appl. Opt. **2,** 1103–1107 (1963).
2. R. Gupta, J. H. Burnett, U. Griesmann, and M. Walhout, "Absolute refractive indices and thermal coefficients of fused silica and calcium fluoride near 193 nm," Appl. Opt **37,** 5964–5968 (1998).
3. E. D. Palik, ed., *Handbook of Optical Constants of Solids* (Academic, San Diego, Calif., 1998), Vols. 1–3.
4. B. N. Taylor and C. E. Kuyatt, "Guidelines for evaluating and expressing the uncertainty of NIST measurement results," NIST Tech. Note 1297 (U.S. Government Printing Office, Washington, D.C., 1994).
5. M. Born and E. Wolf, *Principles of Optics,* 7th ed. (Cambridge U. Press, Cambridge, UK, 1999), pp. 190–193.
6. D. Tentori and J. R. Lerma, "Refractometry by minimum deviation: accuracy analysis," Opt. Eng. **29,** 160–168 (1990).
7. E. C. Y. Inn, "Vacuum ultraviolet spectroscopy," Spectrochim. Acta **7,** 65–87 (1955).
8. D. B. Leviton, J. G. Hagopian, P. H. Geithner, R. A. Boucarut, T. J. Madison, R. A. M. Keski-Kuha, G. Hartig, L. D. Gardner, and T. A. French, "Measuring efficiency of far ultraviolet optical systems in gaseous nitrogen," Opt. Photon. News Suppl. **8,** 1–2 (1997).
9. U. Griesmann, R. Kling, J. H. Burnett, L. Bratasz, and R. A. Gietzen, "The NIST FT700 vacuum ultraviolet Fourier transform spectrometer: applications in ultraviolet spectrometry and radiometry," in *Ultraviolet Atmospheric and Space Remote Sensing: Methods and Instrumentation II,* G. R. Carruthers and K. F. Dymonds, eds., Proc. SPIE **3818,** 180–188 (1999).
10. K. P. Birch and M. J. Downs, "An updated Edlén equation for the refractive index of air," Metrologia **30,** 155–162 (1993).
11. E. R. Peck and B. N. Khanna, "Dispersion of nitrogen," J. Opt. Soc. Am. **56,** 1059–1063 (1966).
12. U. Griesmann and J. H. Burnett, "Refractivity of nitrogen gas in the vacuum ultraviolet," Opt. Lett. **24,** 1699–1701 (1999).
13. C. J. Sansonetti, J. Reader, and K. Vogler, "Precision measurement of wavelengths emitted by a molecular fluorine laser at 157 nm," Appl. Opt. **40,** 1974–1978 (2001).
14. J. Pastrnak and K. Vedam, "Optical anisotropy of silicon single crystals," Phys. Rev. B **3,** 2567–2571 (1971).
15. V. M. Agranovich and V. L. Ginzburg, *Crystal Optics with Spatial Dispersion, and Excitons,* 2nd ed. (Springer-Verlag, New York, 1984).
16. J. H. Burnett, Z. H. Levine, and E. L. Shirley, "Intrinsic birefringence in calcium fluoride and barium fluoride," Phys. Rev. B **64,** 241102 (2001).
17. G. Ghosh, ed., *Handbook of Thermo-Optic Coefficients of Optical Materials with Applications* (Academic, San Diego, Calif., 1998).